Cycloid Drives With Machining Tolerances*

J. G. Blanche
Member of Technical Staff.
Hughes Aircraft Company,
Los Angeles, CA 90009

D. C. H. Yang
Associate Professor.
Mechanical, Aerospace and Nuclear Engineering Department,
University of California,
Los Angeles, CA 90024-1597
Mem. ASME

The cycloidal speed reducer, or cycloid drive, is an epicyclic gear train in which the profile of the planet gear is an epitrochoid and the annular sun gear has rollers as its teeth. The cycloid drive has very high efficiency and small size, in comparison with a conventional gear mechanism, making it an attractive candidate for limited space applications. On the other hand, in this type of transmissions there exist two major drawbacks, namely, backlash and torque ripple. Backlash, the angle through which the output shaft can rotate when the input shaft is held fixed, has a degrading effect on the output accuracy. Torque ripple, the variation in mechanical advantage as the input shaft rotates, causes vibrations and could lead to dynamic instability of the machinery. If the cycloid drive were manufactured to the ideal dimensions, there would be no backlash nor torque ripple. However, in reality, there will always be some machining tolerances. In this paper an analytical model is developed which models the cycloid drive with machining tolerances. Consequently, the effect of machining tolerances on backlash and torque ripple are investigated. It is found that both the backlash and the torque ripple are inherent periodic functions of the input crank angle.

I Introduction

The cycloid drive is an epicyclic gear train which consists of an input shaft with an eccentrically mounted planet gear (Fig. 1). The profile of the planet gear is an epitrochoid which will be discussed later in this paper. The planet gear engages an annular sun gear which has cylindrical rollers as its teeth. The resulting motion of the planet gear is a compound motion. The planet gear orbits about the center of the input shaft due to the eccentricity of the input shaft. At the same time, the planet gear rotates about its own center, in the opposite direction from the input shaft rotation, due to engagement with the sun gear. This wobble motion is converted to pure rotary motion of the output shaft by a constant velocity joint. The constant velocity joint consists of pins attached to a plate which is fixed to the output shaft. These pins engage holes, in the planet gear, which are larger in radius by an amount equal to the amount of offset in the input shaft. The clearance between the pins and the holes allows the planet gear to translate around the input shaft while transmitting only the rotary motion to the output shaft.

Typically the cycloid drive contains two planet gears which are shifted 180 degrees from each other on the input shaft to provide dynamic balancing. It can be seen from this description of the cycloid drive that all contact within the mechanism is rolling contact as opposed to the sliding contact which occurs in a conventional gear mechanism. This has the effect of reducing the heat generated within the mechanism and thereby increasing the efficiency. Efficiencies as high as 95 percent have been realized with the cycloid drive [1]. The unique tooth design in the cycloid drive enable it to achieve very high gear ratios (from 11 to 87) in a single stage. High efficiency and small size are the main characteristics which make the cycloid drive an attractive candidate for many applications.

Although some researchers on mechanical systems and drives with tolerances were reported [2–9], not many studies concerned gear cycloid drives. Botsiber and Kingston [8] describe, with little analytical work, the theory of operation of the cycloid drive mechanism. Pollitt [9], with more analytical detail, shows how to find the point of contact between the planet gear and the pins in the sun gear and concludes that the number of pins required in the sun gear is one more than the gear ratio.

In many industrial applications of cycloid drive, often, two problems of practical importance appear: the existence of

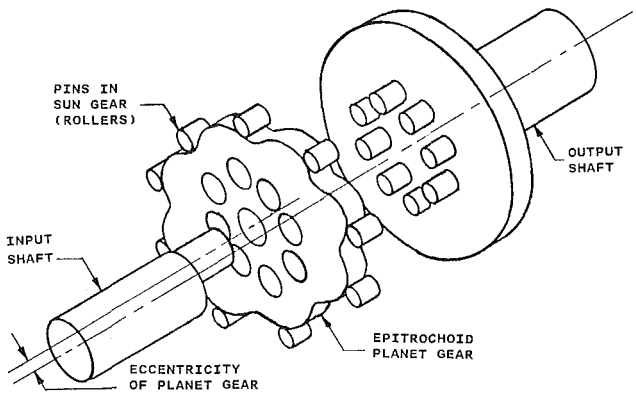

Fig. 1 Exploded view of cycloidal speed reducer

*Based in part on the thesis of the first author in partial fulfillment of the requirements of the Masters degree in the Mechanical, Aerospace, and Nuclear Engineering Department, UCLA, 1986.

Contributed by the Design Automation Committee for publication in the JOURNAL OF MECHANISMS, TRANSMISSIONS, AND AUTOMATION IN DESIGN. Manuscript received July 1988.

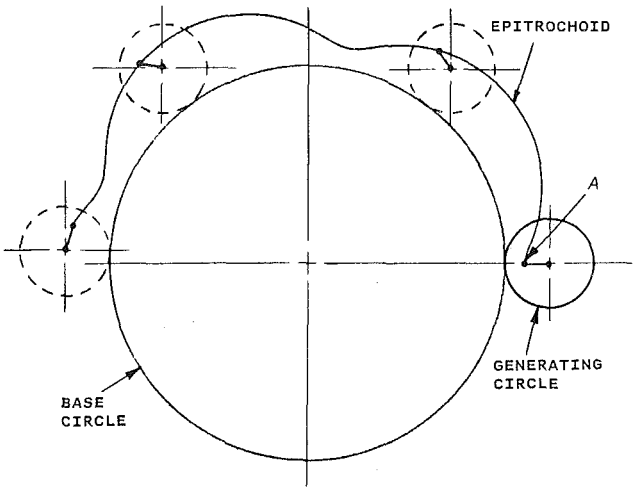

Fig. 2 Epitrochoid being generated

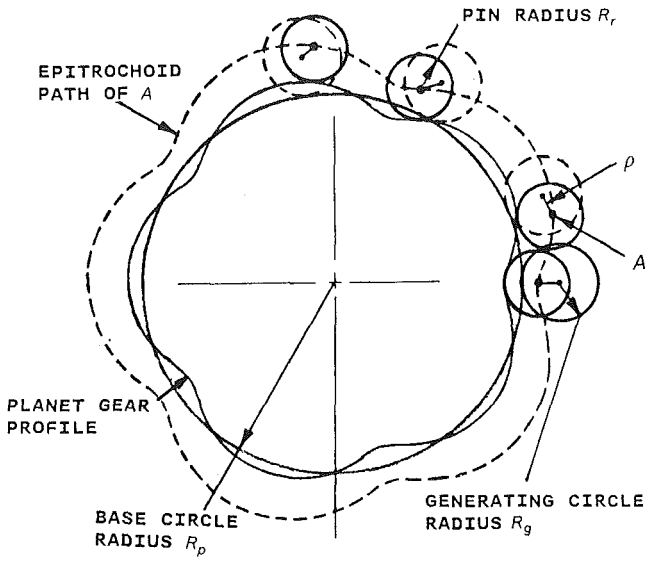

Fig. 3 Epitrochoid planet gear

backlash and torque ripple. Backlash in the cycloid drive is due to machining tolerances, and is sometimes necessary for lubricating tooth surfaces and preventing jamming situations. However, backlash also results in additional dynamic forces, reduced stability and inherent noise and vibration particularly in high speed and frequent stop-start operation as in the joint transmission of an industrial robot. The second problem, torque ripple, is defined as the variation in the gear ratio of the transmission as the input shaft rotates. If the gear ratio varies as the input shaft rotates, a constant input torque (angular velocity) will result in a varying output torque (angular velocity). The results of this torque ripple could range from small vibrations to harmonic resonance of the machinery. In this paper by using complex vectors and homogeneous transformations we develop an analytical model including the consideration of machining tolerance and its effects on the backlash and torque ripple. The interrelationships among machining tolerance, backlash, and torque ripple are then determined via computer-aided procedures.

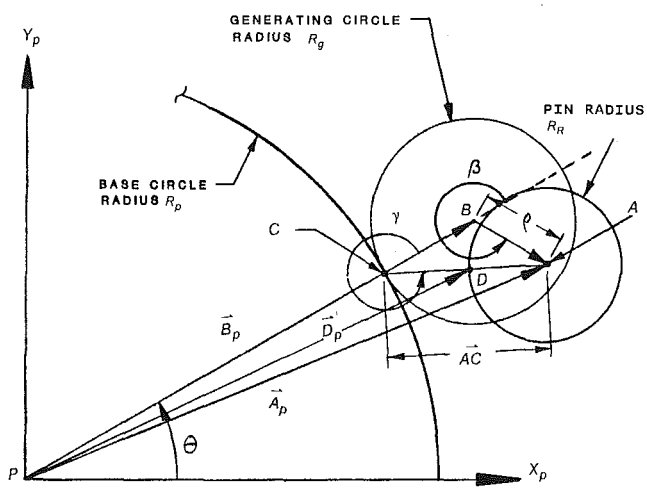

Fig. 4 Location of contact point PC

II Kinematic Model of Ideal Cycloid Drives

The following is a discussion of the formulas which describe the ideal cycloid drive, i.e., one manufactured without any machining tolerance. The formulas derived in this section are in complex vector notation which is used in order to make the logic flow more obvious and is believed to have advantages in simplicity and consistency in the derivations.

The first step to begin the development of the numerical model of the cycloid drive is to develop the equations which define the profile of the planet gear.

The epitrochoid is a member of the family of curves known as cycloids. Referring to Fig. 2, a cycloid is generated by the trace of a point A, which is attached to a circle, known as the generating circle, which rolls without slipping around the outside of a fixed circle, known as the base circle. When the point A lies on the interior of the generating circle, the curve which is generated is known as an epitrochoid. Furthermore, if the ratio of the radius of the base circle (R_p) to the radius of the generating circle (R_g) is an integer, the curve will be closed with R_p/R_g lobes, as shown by the dashed curve in Fig. 3. Now let us attach the center of a roller of radius R_r to the point A as A traces the closed epitrochoid curve. The envelope of all roller positions will be a smaller epitrochoid curve which is equidistant from the original curve by the amount R_r. This smaller curve, as shown by the solid curve in Fig. 3, is the ideal profile of the planet gear, and R_r is the radius of the cylindrical rollers which make up the teeth (pins) of the sun gear as shown in Fig. 1.

Referring to Fig. 4, let PX_pY_p define a coordinate frame attached to the center of the planet gear. We can define the location of the point of contact D_P as follows.

$$\bar{D}_P = R_p e^{i\theta} + (|AC| - R_r)e^{i(\theta+\gamma)} \tag{1}$$

where $|AC| = (R_g{}^2 + \rho^2 - 2R_g\rho\cos(\theta R_p/R_g))^{1/2}$,

$\gamma = \tan^{-1}(\rho\sin(\theta R_p/R_g)/(R_g - \rho\cos(\theta R_p/R_g)))$,

ρ = distance from the center of the generating circle to the point A,

θ = angle between B_p and X_p-axis.

The roller position, defined by

$\bar{A}_p$, can be derived as

$$\begin{aligned}\bar{A}_P &= (R_p + R_g)e^{i\theta} + pe^{i(\theta+\beta)} \\ &= (R_p + R_g)e^{i\theta} - pe^{(i\phi(1+R_p/R_g))} \\ &= (R_P + R_g)e^{i\theta} - \rho e^{i(\phi(1+R_p/R_g))}\end{aligned} \tag{2}$$

where, $\phi = \theta - 2\pi N/(1+R_p/R_g)$, and N is an integer indicating the sequence of the ring gear and having a range $1 \leq N \leq 1 + R_p/R_g$.

Equation (2) shows that regardless of the location of the first interval, if there are $1 + R_p/R_g$ equal intervals, all of the

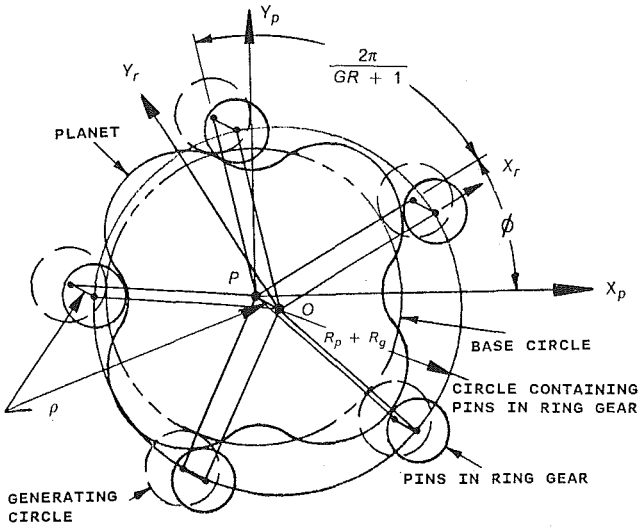

Fig. 5 Ring gear mating with planet gear in position ϕ

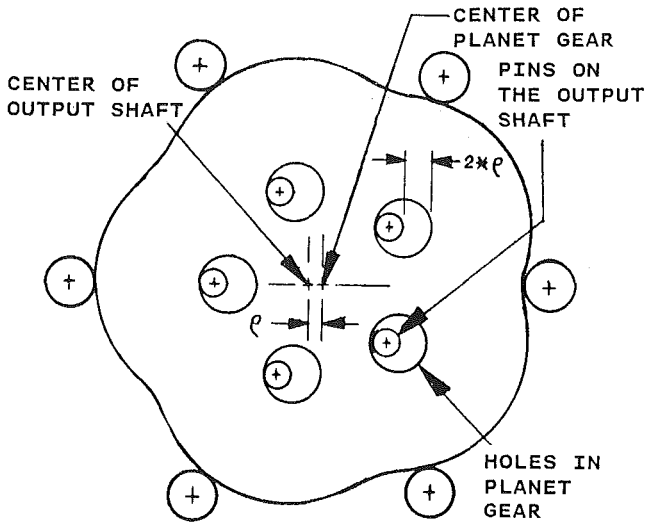

Fig. 6 Constant velocity joint consisting of pins and holes

roller positions will lie in a circle of radius $R_p + R_g$ with its center located by the complex vector

$$-\rho e^{i(\phi(1+R_p/R_g))} \tag{3}$$

relative to the center of the planet gear. A ring gear, of radius $R_P + R_g$, can be constructed with $1 + R_p/R_g$ cylindrical rollers, with radius R_r (referring to Fig. 5). If this ring gear were then placed around the epitrochoid (planet) gear, whose profile is described by equation (1), the rollers could move along the epitrochoid profile keeping in constant contact with the surface. Equation (3) shows that the center of this ring gear would move around the center of the (planet) gear in a circular path of radius ρ.

The cycloid drive is actually a kinematic inversion of the system just described. The annular sun gear is held stationary, while the planet gear is driven by a crank of length ρ which rotates about the center of the sun gear (this is the eccentric input shaft). Figure 5 shows that if a fixed reference frame (X_r, Y_r) is attached to the center of the sun gear with the X-axis passing through the first roller position, a rotation of the crank by an amount $\phi(R_p/R_g)$ relative to this reference frame will result in a rotation of the planet gear by an amount ϕ in the opposite direction. The gear ratio for this mechanism is therefore R_p/R_g. A schematic diagram of this type of drive converting from Fig. 5 is depicted in Fig. 6.

III Kinematic Model with Machining Tolerances

The above discussion is for a cycloid drive which is manufactured to the ideal dimensions. In this section we start to consider how machining tolerances will be modeled. The cycloid drive has many possible locations for clearances due to machining tolerances. In this study we assume that all tolerances are reflected as to the machining tolerance in the profile of the epitrochoid planet gear.

3.1 Planet Gear Profile. If the planet gear profile were larger than the ideal, the mechanism could not be assembled. This is apparent from the previous discussion in which the ideal profile resulted in all of the rollers in contact with the gear surface simultaneously. Therefore machining tolerances will be modelled as a uniform reduction in the profile of the planet gear from the ideal. This profile can be generated using equation (1) with a roller which is larger than the ideal radius R_r by some amount of tolerance. That is, equation (1) becomes:

$$\bar{NI} = R_p e^{i\theta} + (|AC| - (R_r + \delta))e^{i(\theta+\gamma)} \tag{4}$$

where δ = machining tolerance
$\bar{NI}$ = vector to the point on the surface of the nonideal planet gear.

This is the equation of the profile on the nonideal planet gear as a function of θ.

3.2 Lag Angle Analysis. In an ideal cycloid drive, the position of the output shaft θ_0 can be related to the input shaft rotation $\Delta\theta_i$ and an initial output position θ_{0i} by the following equation

$$\theta_0 = \theta_{0i} - \Delta\theta_i/r$$

where r stands for the gear ratio and the negative sign results from the fact that the output shaft rotates in the opposite direction from the input shaft. In a cycloid drive which is manufactured with some machining tolerance, the clearance in the mechanism will allow the input shaft to rotate some finite amount before the output shaft begins to rotate. Therefore the actual position of the output shaft will lag behind the ideal position of the output shaft. Since we are assuming the only tolerance in the mechanism exists in the planet gear profile, this means that the actual position of the planet gear will lag behind the ideal position of the planet gear. Referring to Fig. 7, the angle between the ideal position of the planet gear and the actual position of the planet gear will be referred to as the lag angle θ_L.

One problem in analyzing the lag angle is that it is not intuitively obvious which pin (roller) of the ring gear will make contact with the planet gear first. It is, however, apparent that the contact pin will change as the crank angle changes. We shall defer the problem of determining the contact pin until later in Section 3.3. For now, we simply assume that the contact pin is known, and the lag angle will be analyzed based on this pin. We will begin by analyzing the system shown in Fig. 7. The crank angle will be described as θ_c and the planet gear will initially be in the position it would assume if its profile were ideal. A fixed reference frame will be attached to the ring gear with the X-axis, X_r, passing through pin one. The crank angle will be expressed relative to this axis. The pins will be numbered 1 through $1 + R_p/R_g$ in a counterclockwise direction. A second reference frame will be attached to the planet gear with the X-axis, X_p, oriented as shown in Fig. 7.

Let $\bar{A}_P$ be the vector from the center of the planet gear to the center of the contact pin. Then an imaginary pin of radius

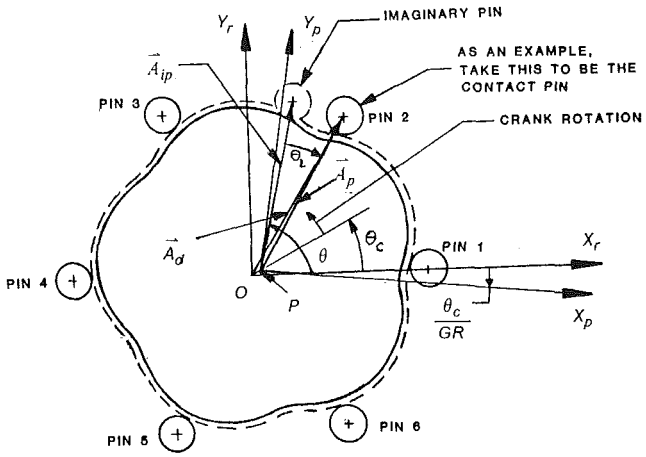

Fig. 7 Coordinate system used for lag angle calculation ---- ideal planet gear profile —— profile with machining tolerance

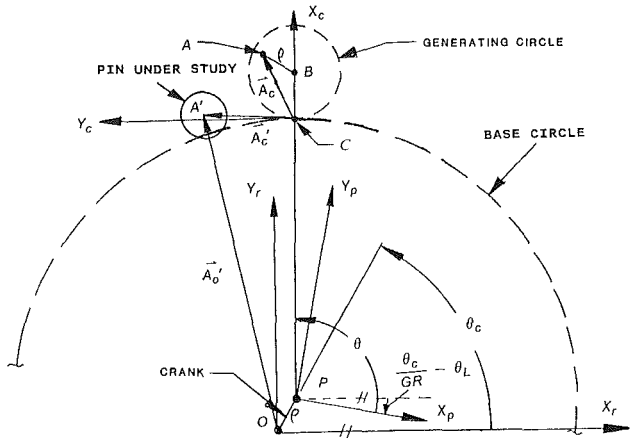

Fig. 8 Coordinate system used for pin distance calculation

R_r is rolled along the surface of the planet gear until the magnitude of the vector describing the location of this imaginary pin ($\bar{\mathbf{A}}_{iP}$), in planet gear coordinates, is equal to the magnitude of the vector locating the actual pin ($\bar{\mathbf{A}}_P$). At this position, the imaginary pin represents the position which the actual pin will have to assume in order for the planet gear to be in contact with it. Referring to Fig. 7, the direction in which the imaginary pin is rolled along the planet gear surface is opposite to the anticipated direction of the lag angle. Since the planet gear rotates in the opposite direction from the crank rotatation, the lag angle will be in the direction of the crank rotation.

The location of the center of the contact pin expressed in ring gear coordinates is

$$\bar{A}_0 = (R_p + R_g)e^{i(2\pi N/(1+r))} \tag{5}$$

where N = (contact Pin Number − 1)

This location in planet gear coordinates, $\bar{\mathbf{A}}_P$, can be identified by first finding the transformation between the coordinates PX_PY_P and OX_rY_r. Let PX_PY_P be defined in OX_rY_r by a homogeneous transformation $[P_0]$, and

$$[P_0] = \text{TRANS}\ (\rho\cos\theta_c,\ \rho\sin\theta_c)\ \text{ROT}\ (Z, -\theta_c/\gamma)$$

where TRANS(a,b) = homogeneous transformation representing a translation of the coordinate system to the position (a, b)

ROT(Z,α) = homogeneous transformation representing a rotation about the Z-axis by an amount α.

When expanding equation (5) in component form yields

$$[P_0] = \begin{bmatrix} 1 & 0 & \rho\cos\theta \\ 0 & 1 & \rho\sin\theta_c \\ 0 & 0 & 1 \end{bmatrix} \begin{bmatrix} \cos(-\theta_c/r) & -\sin(-\theta_c/r) & 0 \\ \sin(-\theta_c/r) & \cos(-\theta_c/r) & 0 \\ 0 & 0 & 1 \end{bmatrix}$$

$$= \begin{bmatrix} \cos(\theta_c/r) & \sin(\theta_c/r) & \rho\cos(\theta_c) \\ -\sin(\theta_c/r) & \cos(\theta_c/r) & \rho\sin(\theta_c) \\ 0 & 0 & 1 \end{bmatrix}$$

From equation (5), the position of the center of the contact pin in the planet gear coordinates is

$$\bar{\mathbf{A}}_P = [P_0]^{-1}\bar{A}_0 = \begin{bmatrix} A_{Px} \\ A_{Py} \\ 1 \end{bmatrix} \tag{6}$$

The next step is to find the location of the center of the imaginary roller $\bar{\mathbf{A}}_{iP}$, as it rolls along the surface of nonideal planet gear. Since the planet gear and the imaginary roller are in contact, they share a common surface normal which passes through the point of contact. In addition, all surface normals of the pin pass through its center. From Fig. 4 we can see that the line which is normal to the surface to the epitrochoid contains a line segment C-A. Therefore, the center of the pin must lie on this line at a distance R_r from the epitrochoide surface. This information, combined with equation (4), yields the following equation for the vector ($\bar{\mathbf{A}}_{iP}$) in terms of θ;

$$\bar{\mathbf{A}}_{iP} = R_p e^{i\theta} + (|\,AC\,| - \delta)e^{i(\theta+\gamma)} = \begin{bmatrix} A_{iPx} \\ A_{iPy} \\ 1 \end{bmatrix} \tag{7}$$

The lag angle analysis then consists of finding the value for θ which satisfies $|\,\bar{\mathbf{A}}_{iP}| = |\,\bar{\mathbf{A}}_P\,|$. This results in the following equation.

$$(A_{iPx}{}^2 + A_{iPy}{}^2)^{1/2} - (A_{Px}{}^2 + A_{Py}{}^2)^{1/2} = 0$$

Substitution of $\bar{\mathbf{A}}_P$ and $\bar{\mathbf{A}}_{iP}$ from equations (6) and (7) yields:

$$(R_p^2 + (|\,AC\,| - \delta)^2 + 2R_p\ (|\,AC\,| - \delta)\cos\gamma)^{1/2} - ((PD/2)^2 + \rho^2 - 2\rho(PD/2)\cos(2\pi N/(1+r-\theta_c))^{1/2} = 0 \tag{8}$$

where, $PD\ (=2(R_p + R_g))$ is defined as the pitch diameter of the planet gear.

When equation (8) is satisfied, the angle from $\bar{\mathbf{A}}_{iP}$ to $\bar{\mathbf{A}}_P$ is the lag angle.

3.3 Pin Distance Analysis. Once the lag angle has been evaluated for a given contact pin (an arbitrary one), it is necessary to know if any of the other pins in the sun gear are also in contact with the planet gear. One way to determine this is to calculate the distance from each pin to the surface of the planet gear. This distance will be measured along the line which is normal to the planet gear profile and passes the center of the pin under study. A third coordinate frame is used in this calculation. This frame is attached to the point of contact, point C, between the generating circle and the base circle. As shown in Fig. 8, the X-axis, X_c, of this coordinate frame lies on a radius of the base circle and points outward from its center. Since the vector ($\bar{A}_C$), normal to the epitrochoide, is in the direction of line C-A, it can be represented in coordinate form as

$$\bar{\mathbf{A}}_C = \begin{bmatrix} R_g - \rho\cos(\theta r) \\ -\rho\sin(\theta r) \\ 1 \end{bmatrix} = \begin{bmatrix} A_{cx} \\ A_{cy} \\ 1 \end{bmatrix} \tag{9}$$

relative to the coordinate frame at C. The transformation from the reference frame C to the ring gear coordinate frame can be found by

$$[C_0] = \text{TRANS}(\rho\cos\theta_c, \rho\sin\theta_c)^*\text{ROT}(Z, \theta+\theta_L - \theta_c/r)^*\text{TRANS}(R_g, 0)$$

where θ_L = Lag Angle
If we let $\alpha = \theta + \theta_L - \theta_c/r$, the matrix form of this equation becomes:

$$[C_0] = \begin{bmatrix} 1 & 0 & \rho\cos\theta_c \\ 0 & 1 & \rho\sin\theta_c \\ 0 & 0 & 1 \end{bmatrix} \begin{bmatrix} \cos\alpha & -\sin\alpha & 0 \\ \sin\alpha & \cos\alpha & 0 \\ 0 & 0 & 1 \end{bmatrix} \begin{bmatrix} 1 & 0 & R_g \\ 0 & 1 & 0 \\ 0 & 0 & 1 \end{bmatrix}$$

$$= \begin{bmatrix} \cos\alpha & -\sin\alpha & R_g\cos\alpha+\rho\cos\theta_c \\ \cos & \cos\alpha & R_g\sin\alpha+\rho\sin\theta_c \\ 0 & 0 & 1 \end{bmatrix}$$

The location of the center of the pin under study relative to the reference frame attached to C is found as follows.

$$\bar{\mathbf{A}}_c' = [C_0]^{-1}\bar{\mathbf{A}}_0' \tag{10}$$

where $\bar{\mathbf{A}}_c'$ represents the position of the vector of $\bar{\mathbf{A}}_0'$ in C coordinates. We are looking for the value of θ for which the vectors $\bar{\mathbf{A}}_c$ and $\bar{\mathbf{A}}_c'$ are in the same direction. When these two vectors are colinear, their cross product will have a magnitude of zero. Therefore, we are looking for the value of θ for which the following equation is satisfied.

$$\bar{\mathbf{A}}_c \times \bar{\mathbf{A}}_c' = 0$$
$$A_{cx}A_{cy}' - A_{cy}A_{cx}' = 0$$

Substituting equations (9) and (10) into the above equations, we have

$$((R_g - \rho\cos(\theta r))(PD\sin(2\pi N/(1+r) - \alpha)/2 - \rho\sin(\theta_c - \alpha)) - (-\rho\sin(\theta r)(PD\cos(2\pi N/(1+r) - \alpha)/2 - R_p - \rho\cos(\theta_c - \alpha)) = 0 \tag{11}$$

Once the value of θ is found for which this equation is solved, the pin distance can be calculated. Recall that vector $\bar{\mathbf{A}}_c$ represents the location of the center of the pin which is used to generate the planet profile. Therefore, the planet surface will be located at a distance

$$|\bar{\mathbf{A}}_c| - R_r - \delta$$

from the point c in the direction of the vector $\bar{\mathbf{A}}_c$. The vector $\bar{\mathbf{A}}_c'$ represents the center of the pin under study. When $\bar{\mathbf{A}}_c$ and $\bar{\mathbf{A}}_c'$ are collinear, the pin distance can be calculated as:

$$\text{PIN DIST} = (|\bar{\mathbf{A}}_c'| - R_r) - (|\bar{\mathbf{A}}_c| - R_r - \delta) = |\bar{\mathbf{A}}'| - |\bar{\mathbf{A}}| + \delta \tag{12}$$

Notice that if the pin distance has a negative value this would require that the pin under study penetrate the surface of the planet gear. This indicates an incorrect choice of the contact pin.

We now can see that the lag angle analysis actually consists of two parts. These are selection of the proper contact pin and calculation of the lag angle. From equations (8) and (11), we can see that this problem does not lend itself well to an analytical solution. Therefore, we have developed an efficient numerical algorithm (presented in Section V) to solve this problem. If a first guess is made for the contact pin, equation (8) can be used as an error function in an iterative search for θ to evaluate the lag angle. Once the lag angle has been evaluated, equation (11) can be used in an iterative search to find the distance between each of the remaining pins and the planet surface. The pin with the minimum distance can be used as a contact pin and the process repeated until the minimum pin distance is slightly greater than or equal to zero.

3.4 Backlash Analysis. When the input shaft is rotating in one direction with a constant speed, the lag angle represents the error in the actual position of the output shaft relative to its ideal position. If the input shaft were to stop, inertia in the system would cause the planet gear to continue to rotate past the ideal position until it contacts the sun gear at some position ahead of the ideal position. Let us call this position the lead angle. The lead angle is calculated in the same way in which the lag angle was calculated except the direction in which the imaginary pin is moved is opposite from the direction in the lag angle analysis. It is important to note that the contact pin will not be the same for the lag angle position of the planet gear as it is for the lead angle position. The backlash is the total range of motion of the planet gear for a given crank angle. Therefore, the backlash is the sum of the lag angle and the lead angle.

IV Torque Ripple (Actual Gear Ratio) Analysis

The ideal gear ratio of the mechanism is the ratio of the radii of the base circle and the generating circle of the planet gear, i.e., R_p to R_g. However, the actual gear ratio as define by the ratio of the input shaft speed to the output shaft speed might differ from the ideal gear ratio if the profile of the planet gear is manufactured with some tolerance. This fluctuation in gear ratio will directly result in output torque variation, though input torque is held constant. This variation of output torque is called torque ripple and is a major concern in practical applications.

Once the proper contact pins has been found and the lag angle has been analyzed, we are interested in finding the gear ratio of the mechanism. Referring to Fig. 9, finding the gear ratio can be accomplished by observing the instantaneous velocity of two points on the planet gear. With the planet gear in contact with the contact pin, we know that the point on the planet gear which is in contact with the pin can only move tangentially to the surface of the pin. Therefore, the normal to the surface of the epitrochoid at the point of contact between the gear and the pin will be normal to the velocity vector of the point on the planet gear surface. Also we know that the center of the planet gear will always have a velocity vector which is normal to the crank due to the motion of the crank. Now we know the direction of the velocities of two points on the planet gear we can find the instantaneous center of rotation of this gear. The instantaneous center will be the intersection of the line defined by the crank and the normal to the planet surface at the point of contact with the contact pin. Referring to Fig. 9, these two lines are defined in the planet coordinate systems by equations (13) and (14), respectively, as

$$Y_1 = \tan(\theta_c + (\theta_c/r) - \theta_L)^*X_1 \tag{13}$$

$$Y_2 = X_2\ \tan(\theta+\gamma) - R_p\sin\theta/\cos(\theta+\gamma) \tag{14}$$

The point of intersection of these lines (I_{Px}, I_{Py}) is found from solutions of equations (13) and (14); and

$$I_{Px} = -R_p\sin\theta/(\cos(\theta+\gamma)^*(\tan(\theta_c(1+1/r) - \theta_L) - \tan(\theta+\gamma))) \tag{15}$$

$$I_{Py} = \tan(\theta_c(1+1/r) - \theta_L)I_x \tag{16}$$

Once the location of the instantaneous center is found the gear ratio can be found by using

$$r_a = \frac{\omega_i}{\omega_o} = \left|\frac{IP}{PO}\right| = \frac{|IP|}{\rho} \tag{17}$$

In this equation, ω_i and ω_o are angular velocities of the input crank and the output planet gear; $|IP|$ is the distance between the instantaneous center and the center of the planet gear; and the subscript "a" is used to differentiate the actual gear ratio of the gear mechanism with tolerance from the ideal gear ratio

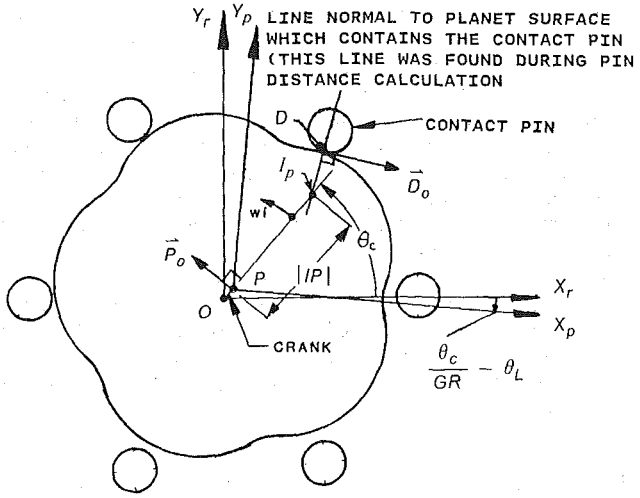

Fig. 9 Coordinate system used for gear ratio calculation

used to generated the profile of the planet gear. By substituting $(I_{Px}^2 + I_{Py}^2)$ provided in equations (15) and (16) for $|IP|$ in equation (17), we will find that the actual gear ratio of this drive is a periodic function of the input crank θ_c.

V Computer-Aided Design Package for Kinematic Analysis

A computer-aided package for kinematic analysis was developed. The package was written in FORTRAN and compiled on an IBM-XT using Microsoft FORTRAN version 3.20. Lotus 123 was then used to interpret the resulting data files and generate the plots.

A flow chart of the basic numerical model is shown in Fig. 10. The first section of the program prompts the user for data to be input from the keyboard. The data which is input describes the ideal gear configuration; pitch diameter, ideal gear ratio and normalized tooth height h (the normalized tooth height is defined as the percentage of tooth height, 2ρ, to the diameter of the generating circle, $2R_g$). The program also prompts the user for the machining tolerance, the crank angle, the direction of rotation of the crank, and the accuracy to be used during the iterative search routines. Once all of this data has been entered, the program makes a first guess at the contact pin. This guess is based on the pin which is closest to being in line with the crank. The lag angle is then calculated for this contact pin.

5.1 Lag Angle Routine. The formula used for calculating lag angle is given by equation (8) in Section 3.2. The search routine is designed to locate the value of θ for which equation (8) is zero. The initial value of θ chosen is the value which would yield zero error if there were no tolerance in the mechanism. From equation (8), we can see that this value is:

$$\theta = 2\pi N/(1+r) + \theta_c/r \qquad (18)$$

where N = (PIN NUMBER − 1)

Figure 11(*a*) shows a typical plot of the error function for values of θ ranging from the initial guess as defined by equation (18) to 2π away from this in the search direction. This figure shows the error function to be periodic with period of $2\pi/r$.

The search routine needs therefore to search in the direction opposite from the direction of crank rotation through only the range defined by $2\pi/r$ instead of an entire 2π. A typical plot of the error function in this range is shown in Fig. 11(*b*). Notice that there are two zeros in this search range. The object of the

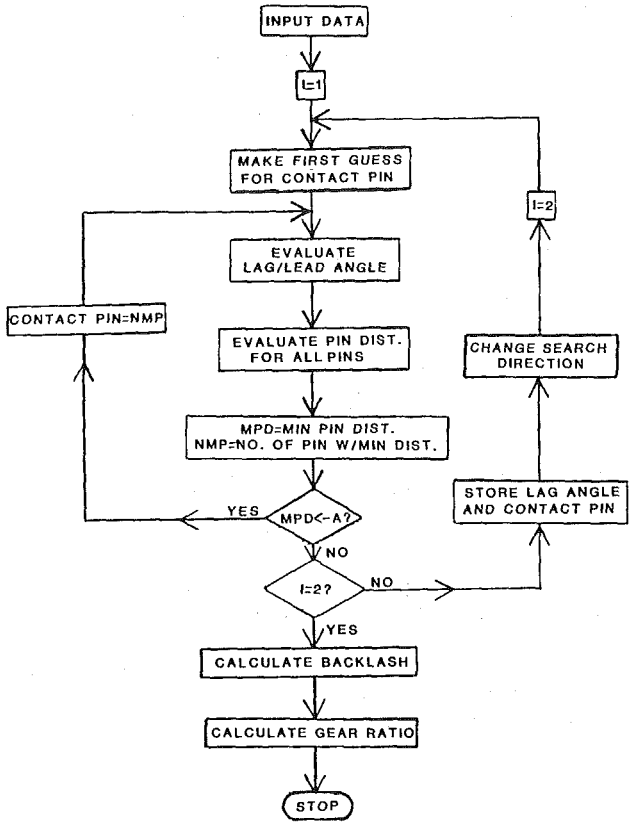

Fig. 10 Flow chart of numerical model

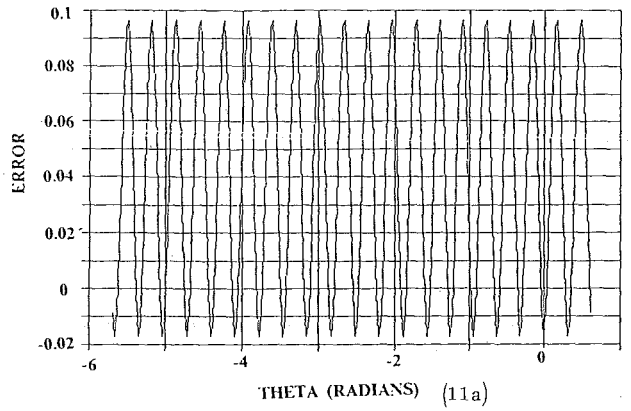

Fig. 11(*a*) θ versus error for the lag angle routine

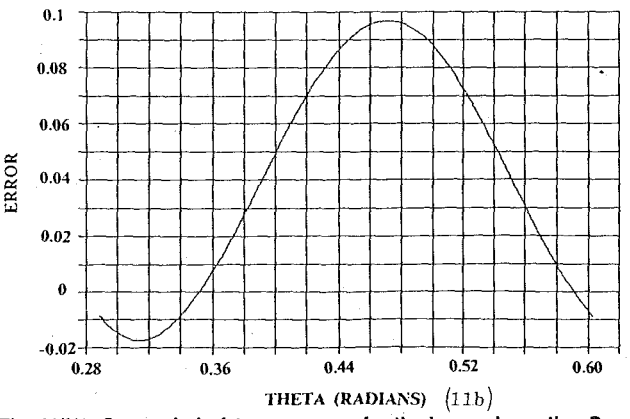

Fig. 11(*b*) One period of θ versus error for the lag angle routine D_p = 4.0 in., r = 20, h = 60, δ = 0.01 in. and the pin under study is pin 3

search routine is to locate the first zero. The search routine begins with θ defined by equation (18). Equation (8) is used to evaluate the error. The angle θ is then incremented by an amount $\Delta\theta$ in the direction of the search and the error is evaluated again. This process is repeated until the sign of the error changes, then Newton's method is used to make successive guesses for θ until the error is within the desired accuracy. The lag angle is analyzed as the angle from $\vec{\mathbf{A}}_{ip}$ *to* $\vec{\mathbf{A}}_p$. Once the lag angle has been evaluated for a given contact pin, the program proceeds to the pin distance routine.

5.2 Pin Distance Routine. The pin distances are calculated with the planet gear in contact with the contact pin. The pin under study is then set to pin number one and the distance is evaluated. The distances from each of the remaining pins to the planet gear are then evaluated. By evaluating the pin distances for all of the pins we get a quantitative measure of the accuracy of the model since the contact pin should have a distance of zero.

The error function used in this routine is equation (11), derived in Section 3.3. As in the lag angle analysis, the first value of θ will be taken to be the angle which would yield a solution if the mechanism had no tolerance. It can be shown by substitution that this initial value will be:

$$\theta = 2N/(1+r) + \theta_c/r \tag{19}$$

A plot of this error function within $2\pi/r$ on both sides of this first guess is shown in Fig. 12. Note that there is only one solution in this neighborhood. The direction of the search routine, relative to the first guess, can be determined from the sign of the error. From the plot of the error function, we can see that if the value of the error is positive, the value of θ must be increased, if the error is negative θ must be decreased. This phenomenon is not unique to this one plot of the error function, but results from the derivation of the error function. Recall that the error function was derived as the cross product of two coplanar vectors. Therefore the sign of the error will give an indication of the relative position of the vectors. The plot of the error function shows that we should get close to the solution before Newton's method is used to make successive guesses. Therefore, the same method is used in this search routine as was used in the lag angle routine. The error is evaluated for the initial guess. The sign of this error determines the direction of the search. The angle θ is then incremented by an amount $\Delta\theta$ in the direction of the search until the error changes sign. Then Newton's method is used to make each successive guess for θ until the error is within the desired accuracy.

Once the value of θ has been found for which the error is within the desired accuracy, the pin distance is evaluated using

$$\text{PIN DIST} = |\vec{\mathbf{A}}_c'| - |\vec{\mathbf{A}}_c| + \delta \tag{20}$$

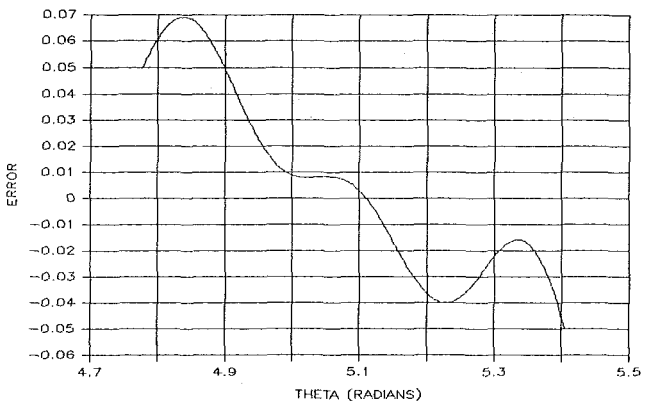

Fig. 12 θ **versus error for the pin distance routine** $D_p = 4.0$ **in,** $r = 20$, $\delta = 0.0001$ **in. and the pin under study is pin 18**

The contact pin is found when it results in minimum pin distance of zero. The lag angle and the corresponding contact pin are then evaluated and stored. The lead angle is evaluated by changing the search direction and repeating the lag angle analysis. The backlash is then evaluated as the total of the lag and lead angles. Finally, the gear ratio is calculated using the lag angle and the contact pin data which were previously stored and equations (15), (16), and (17) derived in Section III.

5.3 Characteristics of Backlash Variation and Torque Ripple. Here we analyzed the effect of crank rotation on the backlash and gear ratio of the mechanism. The intent was to determine the kinematic characteristics of the backlash variation and the torque ripple. The backlash and gear ratio were analyzed at 300 equal intervals of crank angle from 0 through 2π. Figure 13 is the plot of the data which resulted from this analysis. From these plots we can see that the magnitudes of backlash [Fig. 13(*a*)] and gear ratio [Fig. 13(*b*)] vary periodically with crank angle. Furthermore, we find that the number of cycles in each of these plots are equal to the number of pins in the sun gear. Therefore, the performance of a particular mechanism only needs to be evaluated for crank angles from 0 through $2\pi/(1+r)$ to get a complete picture of its backlash and effective torque ripple.

Figure 14(*a*) is a plot of backlash for crank angles from 0 through $2\pi/(1+r)$. Note that there are two peaks in this range. To explain, we first look at the components which make up the backlash. Recall that the backlash is the total of the lag angle and the lead angle at a given crank position. Furthermore, recall that the contact pins for these two angles are different. Figure 14(*b*) shows the plots of the lag angle and lead angle for the same range of crank rotation used in Fig. 14(*a*). The fact that each component (lag angle or lead angle) of the backlash has a peak which occurs at a different crank angle accounts for the two peaks.

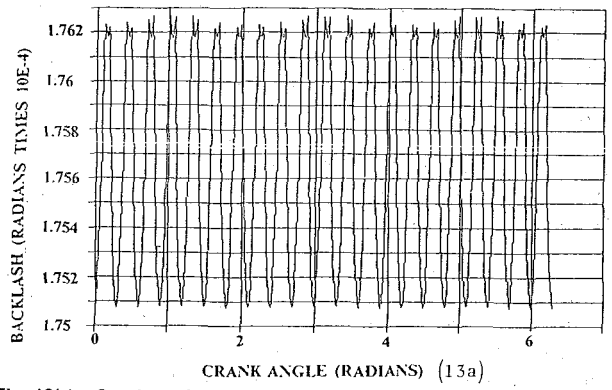

Fig. 13(a) Crank angle versus backlash for one revolution of the crank

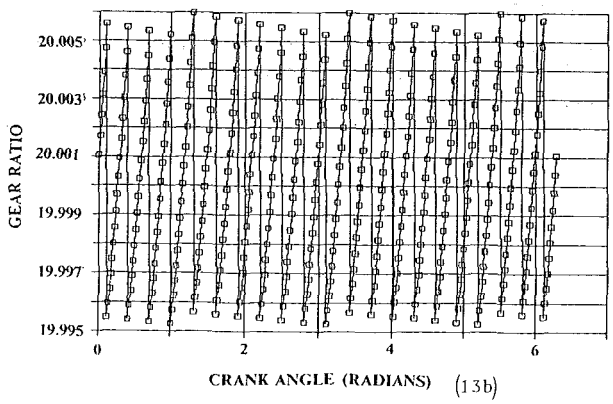

Fig. 13(b) Crank angles versus actual gear ratio for one revolution of the crank $D_p = 4.0$ **in.,** $r = 20$, $h = 60$, $\delta = 0.01$ **in. and error** $= 1.8E-13$

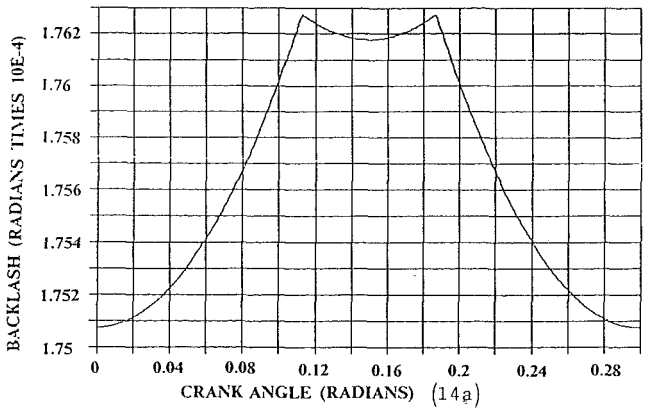

Fig. 14(*a*) One period of crank angle versus backlash

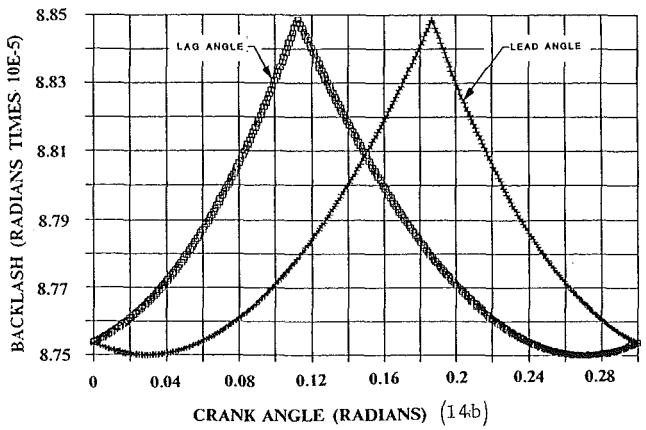

Fig. 14(*b*) Crank angle versus backlash components

Figure 15 shows a plot of the actual gear ratio for crank angles from 0 through $2\pi/(1+r)$. Comparing Figs. 14(*a*) and 15, it is interesting to find that the peak in the lag angle plot coincides with the discontinuity in the gear ratio plot. This is because the peak in the lag angle plot occurs at the crank angle which coincides with the change of the contact pin; consequently, at this moment, the instantaneous center of the planet gear used for calculating gear ratio will change its location discontinuously. In short, the gear ratio varies almost linearly with the crank angle and with a discontinuity at the crank angle corresponding to the change of the contact pin. This finding is important, for it tells that a cycloid drive has an inherent noise source, the torque ripple, with a frequency proportional to the input shaft frequency. More precisely, it is the multiplication of number of pins and the input frequency, i.e., $(1+r)*f_i$, where f_i denotes the input frequency.

VI Concluding Remarks

In this research, we have performed an in-depth kinematic analysis of cycloid drives with machining tolerances. Given a cycloid drive, the relationships among tolerance, backlash, gear ratio, number of rollers, and the size of the planet, gear,

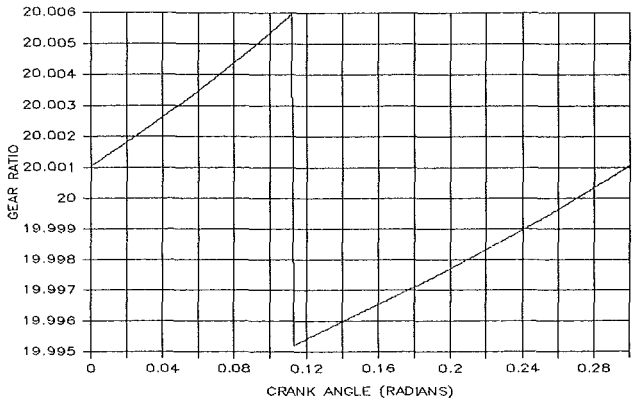

Fig. 15 One period of crank angle versus actual gear ratio

etc. are analytically derived. For an ideal cycloid drive (no tolerance), there is no backlash and the gear ratio equals a constant. However, it is found that for drives with machining tolerance, backlash appears. Moreover, both the backlash and the gear ratio are no longer constants; they become periodical functions of the input crank angle. Based on this model a computer-aided-design package is developed, which enables us to numerically determine the magnitude of the backlash as a function of the drive's design parameters including machining tolerance. Also we find the torque ripple caused by a tolerance is in a form of a periodic excitation noise whose frequency is equal to the frequency of the input shaft times the number of teeth in the ring gear. We believe that the results presented in this paper would be useful in design, analysis and application of this type of transmission devices.

Acknowledgment

The authors are grateful for research support from the UCLA Academic Senate through grant #3847.

References

1 Sumitomo Machinery Corporation S. M. Cyclo Catalog, Seven Malcolm Avenue, Teterboro, N.J.

2 Dubowsky, S., and Freudenstein, F., "Dynamic Analysis of Mechanical Systems with Clearances, Part 1: Formulation of Dynamic Model," ASME *Journal of Engineering for Industry*, Vol. 93, February 1971, pp. 305-309.

3 Dubowsky, S., and Freudenstein, F., "Dynamic Analysis of Mechanical Systems With Clearances, Part 2: Dynamic Response," ASME *Journal of Engineering for Industry*, Vol. 93, February 1972, pp. 310-316.

4 Azar, R. C., and Crossley, F. R. E., "Digital Simulation of Impact Phenomenon in Spur Gear System," ASME *Journal of Engineering for Industry*, Vol. 99, August 1977, pp. 792-798.

5 Dubowsky, S., and Gardner, T. N., "Design and Analysis of Multilink Flexible Mechanism with Multiple Clearance Connections," ASME *Journal of Engineering for Industry*, Feb. 1977, pp. 88-96.

6 Kim, M. R., and Newcombe, W. R., "The Effect of Cam Profile Errors and System Flexibility on Cam Mechanism Output," *Mechanism and Machinery Theory*, Vol. 17, No. 1, 1982, pp. 57-72.

7 Yang, D. C. H., and Sun, Z. S., "A Rotary Model for Spur Gear Dynamics," ASME JOURNAL OF MECHANISMS, TRANSMISSIONS, AND AUTOMATION IN DESIGN, 85-DET-2, 1985.

8 Botsiber and Kingston, L., "Design and Performance of the Cycloid Speed Reducer," *Machine Design*, June 28, 1956, pp. 65-69.

9 Pollitt, E. P., "Some Applications of the Cycloid Machine Design," ASME *Journal of Engineering for Industry*, November 1960, pp. 407-414.